

Investigation of Distinction Chemical Markers for Rhubarb Authentication Based on High-Performance Liquid Chromatography-Time-of-Flight Mass Spectrometry and Multivariate Statistical Analysis

Shuzhen Xu¹ · Gongjun Yang^{1,2} · Fang Feng^{1,2,3} 

Received: 12 February 2017 / Accepted: 23 May 2017 / Published online: 20 June 2017
© Springer Science+Business Media New York 2017

Abstract Rhubarb is a famous herb medicine commonly used for the treatment of purgation, anticancer, anti-inflammation, and promoting blood circulation in clinical. Recently, the situation that unofficial rhubarb is confused with official one on the market is becoming a serious threat to the efficacy of the crude drug. In this study, a comprehensive approach using principal component analysis (PCA) and orthogonal partial least squares discriminant analysis (OPLS-DA) based on liquid chromatography coupled with electrospray ionization time-of-flight mass spectrometry and diode-array detection was established to explore novel markers for rhubarb authenticity which is important for quality assurance, pharmaceutical activity, and market protection. The method was validated based on pooled quality control samples and was found reliable and repeatable. In the procedure, metabolic fingerprinting of official and unofficial samples from different geographic regions was analyzed, and a total of 35 phenolic compounds were screened out and were tentatively characterized as authenticity markers of rhubarb based on their mass spectra and UV spectra. The content and pharmacological activity difference of these ingredients belonging to

different compound classes (such as anthraquinone glycosides, catechins, stilbenes, naphthalenes, and butyrophenones) were compared by compound types on the base of extracted ion chromatograms. And anthraquinone glycosides, which have been considered as the major purgative components of rhubarb, were relatively contained more in official rhubarb. This research proved that a chemometric method based on liquid chromatography with diode-array detection and time-of-flight tandem mass spectrometry can comprehensively analyze chemical variation and provide evidence for quality control of herbal medicine.

Keywords HPLC-TOF-MS · Chemical markers · Official and unofficial rhubarb · PCA · OPLS-DA

Introduction

Rhubarb, one of the most famous herb medicines in China, is recorded in 26 and 16 clinical commonly used prescriptions in Shanghan Lun and Golden Chamber for its obvious therapeutic effects on the treatment of purgation, anticancer, anti-inflammation, and promoting blood circulation, especially for its distinguished pharmacological activities of purgation (Jelassi et al. 2013; Suboj et al. 2012; Bajic et al. 2016). Besides, around the world, rhubarb has been used as medicinal materials for thousands of years and has been documented in European Pharmacopeia, British Pharmacopeia, and Japanese Pharmacopeia for long. According to the regulation of Chinese pharmacopeia, in the assay of purity in Chinese pharmacopeia, rhaponticin belongs to stilbene category and is prohibited to be detected in official rhubarb by thin-layer chromatography since unofficial rhubarb contains high amount of it (Chinese Pharmacopoeia commission 2015). However, large market demand, multi-source characteristic, and

✉ Gongjun Yang
ggyang@cpu.edu.cn

✉ Fang Feng
fengfang1@hotmail.com

¹ Department of Pharmaceutical Analysis, China Pharmaceutical University, TongJiaXiang No. 24, Nanjing 210009, People's Republic of China

² Key Laboratory of Drug Quality Control and Pharmacovigilance (Ministry of Education), China Pharmaceutical University, Nanjing 210009, China

³ Center for Drug Quality Evaluation, China Pharmaceutical University, Nanjing 210009, China

complex composition of rhubarb have provided principal incentives for the use of unofficial rhubarb, such as *Rheum franzenbachii* Munt. and *Rheum japonicas* Hoult., which are informally called Shandahuang (SDH) and Tudahuang (TDH) in folk, respectively. It has been reported that SDH contains high content of stilbenes and tannins, and the principal components of TDH are naphthalenes and tannins (Li et al. 2012; Zhu et al. 2008). The mainly pharmacological activities of stilbenes, naphthalenes, and tannins are anti-cancer, anti-inflammatory, antioxidant, and antimicrobial (Lastra and Villegas 2005; Santana et al. 2015; Chung et al. 1998). Pervious study showed that the anthraquinone parts act as the pharmacophore to inhibit adrenergic receptor, and the glycosyl plays the carrier's role to protect the active parts until they reach the large intestine. Thus, the purgative activities of unofficial rhubarb are much weaker since anthraquinone glycosides are the main purgative components of DH (Feng et al. 2013). What is more, SDH showed heavier toxicity than DH in vivo acute toxicity test and in vitro cytotoxicity essay (Feng et al. 2012). Therefore, developing a method to inspect the mix or misuse unofficial rhubarb is crucial for the safe and effective usage of rhubarb.

In a previous report, Pang Yu et al. developed a high-performance liquid chromatography (HPLC) fingerprint combined with principal component analysis (PCA) and cluster analysis method to distinguish official and unofficial rhubarb (Pang et al. 2014). However, the different components among different species are still undefined; so, a comprehensive and time efficient approach to investigate the component diversity is very necessary for rhubarb quality control. Considering the various components, LC-MS is more appropriate to simultaneously analyze rather complex compounds in herb medicines (Cai et al. 2002) since HPLC have some limitations such as low sensitivity, poor resolution, and limited detection. The accurate mass value and adjustable fragment voltages offered by TOF-MS provide abundant information for compound structure deduction and confirmation. To date, LC-MS has been increasingly used for chemical profiling and quality control of Chinese medicine herbs (Ye et al. 2007; Zhang et al. 2015). Unfortunately, traditional Chinese medicine is a complex mixture, and it is difficult and time-consuming to identify every chemical compound in the procedure of quality control and improper to select one or a few compounds to be the representative. Therefore in combination with chemometric analysis, complicated components could be systematically analyzed and simplified into a series of chemical markers with greater content difference, and then to explore the changes of chemical composition, control the quality of herbs, and so on. The main advantage of metabolomics in authentication is its untargeted nature, which enable the inspection of emerging frauds. Thus, the aim of this work was to investigate, for the first time, the potential of an untargeted metabolomic approach developed using liquid chromatography coupled to

high-resolution MS (LC-TOF) to explore the quality and authenticity of rhubarb.

In the current study, a multivariate statistical analysis based on HPLC-DAD-TOF-MS was developed to comprehensively investigate the differences between components in official rhubarb and unofficial rhubarb and accurately identify these compounds, without the help of any reference substances. To find out the chemical markers, pairwise comparisons between DH vs SDH and DH vs TDH were performed by the means of chemical profiles and chemometric methods including PCA and OPLS-DA. To provide an intuitive comparison and validation, validation ions were extracted from their total ion chromatograms (TICs) and then combined to form extracted ion current chromatograms (EICs) so that the content of chemical markers were compared based on relative peak areas.

Materials and Methods

Reagents and Herbal Materials

Methanol of HPLC grade and acetic acid were purchased from Merck (Darmstadt, Germany) and Sigma Chemical (St. Louis, USA), respectively. Ultra high purity water was prepared using a Millipore-Q water purification system (Bedford, USA).

Eight batches of official rhubarb (NO. S1-S8) and 13 batches of unofficial rhubarb including SDH (NO. S9-S13) and TDH (NO. S14-S21) were purchased from different Chinese herbal medicine markets and hospitals located in Anhui, Shanxi and Hubei Province of China during December 2015 to May 2016, and were authenticated by Professor Minjian Qin (Department of Chinese Materia Medica, China Pharmaceutical University, Nanjing, China).

Sample Preparation

All the samples (NO. S1-S21) were ground into powder and passed through a 40 mesh (0.45 mm) sieve. An accurately weighed powder (1.2 g) was extracted by ultrasonication with 10 mL methanol/water (70:30, v/v) using a KQ-3200E sonicator (Kunshan Ultrasonic sonicator company, China) at 120 W for 40 min, at room temperature. The extract solution was filtered through 0.22- μ m micropore films for analysis.

HPLC-DAD-TOF/MS Conditions

The analysis was performed on an Agilent-1260 LC system coupled to an Agilent-6230 Time-of-Flight mass spectrometer (Agilent, Santa Clara, CA, USA) via an electrospray ionization interface. Chromatographic separation was performed on a Lichrospher C₁₈ column (250 mm \times 4.6 mm, 5 μ m, Hanbon, China). The mobile phase consisted of 0.2% acetic acid in water (A) and methanol (B), with a flow rate of 1.0 mL/min.

The following gradient was used: 0–10 min 5–12% B, 10–28 min 12–26% B, 28–53 min 26–38% B, 53–70 min 38–42% B, 70–80 min 42–47% B, 80–88 min 47–51% B, 88–130 min 51–71% B, 130–135 min 71–100% B, 135–140 min 100–60% B, and 140–145 min 60–5% B. Injection volume and column temperature were 20 μL and 35 $^{\circ}\text{C}$, respectively. The wavelength range of DAD scan was set at 200–600 nm.

The mass spectrometer was performed in both positive and negative mode with a scanning range of m/z 100–1100 Da in full scan mode. The ionization source conditions were set as follows: nebulizing gas and drying gas were nitrogen at 350 $^{\circ}\text{C}$ with the flow rate of 10.0 L/min and the pressure of 30 psig, respectively. The capillary voltage of positive and negative mode was 4000 and -3500 V, respectively. In order to investigate the influence of fragment voltage to fragment ions, fragmentor after sample capillary was at a series of 135v, 175v, 225v, 300v, and 375v. Before injection, mass value was calibrated with tuning solution to an extent of less than 2 ppm bias. During the procedure of analysis, reference solutions containing ions of m/z 112.985587 and 1033.988109 were used to maintain the accuracy of measured ions in negative mode.

Data Processing and Chemometrics Analysis

The raw global MS data were loaded into XCMS online platform for feature detection, retention time correction, alignment, and the extraction of peak intensities (Smith et al. 2006). For different batches of the same species of rhubarb, filter was conducted by choosing the data with RSD below 35%. Each ion intensity was weighed by unit variance to eliminate the discrimination of variables. After normalization, ions and its number were imported into SIMCA-P software (13.0 demo version, Umetrics, Sweden) for PCA and OPLS-DA. Unsupervised PCA was employed to estimate the clustering degree of several batches of rhubarb. Supervised OPLS-DA combined with variance cross-validated predictive residuals (CV-ANOVA) $p < 0.01$ was applied to screen out potential chemical markers among DH, SDH, and TDH. The parameter $Q^2 > 0.5$ is admitted for good predictability of PCA and OPLS-DA models (Triba et al. 2015).

Method Validation

The pooled QC sample prepared by mixing 50 μL of all samples was used to validate sample stability and method repeatability and injection precision. Before batch test, the precision of method was validated by successive analysis of the same QC sample solution five times. In the meantime, sample stability was validated at the time of 0, 3, 6, 9, 12, and 24 h. In the procedure of batch test, QC sample was injected every five samples to measure the change of ion intensity of each compound and the conditions of instrument.

Results and Discussion

Optimization of Extraction Method and LC-TOF-MS Method Development

To achieve the best extraction efficiency, ultrasonic extraction and reflux extraction were conducted and compared to obtain higher extraction efficiency and better reproducibility. Different extraction times (including 30, 40, and 60 min) were also explored in parallel. Combined with previous study on sulfur-fumigated rhubarb in my laboratory (Yan et al. 2016), it was found that ultrasonic extraction 40 min with 70% methanol provided comprehensive information about the composition of official and unofficial rhubarb.

Besides, mobile phase composition, elution conditions, and TOF-MS parameters have been optimized to reduce ion suppression in ionization source and improve resolution to achieve highly efficient separation of multiple phenolic compositions, which was vitally important for the comprehensive chemical profiling of a complex system. By comparison, mobile phase consisting of 0.2% acetic acid aqueous solution and methanol was selected to improve peak shape and enhance ionization efficiency in negative mode. Considering separation efficiency, gradient elution was more suitable to separate complex coexistent substances in rhubarb for high separation efficiency. To get more fragments and further validate the structures of compounds, TOF-MS fragmentor parameter was set as a series, i.e., from 135 to 375 V. The satisfactory HPLC-TOF-MS conditions are detailed in section “HPLC-DAD-TOF/MS Conditions.” Under the optimized conditions, over 50 peaks were detected and separated well in three kinds of samples.

Method Validation

According to six TICs of QC sample, the RSD of ion intensity of ten common peaks 4, 5, 8, 22, 24, 27, 29, 31, 34, and 35 were calculated to evaluated injection precision and sample stability. The results showed that all of the variations were not more than 5%. To assure the reliability of nontargeted metabolomic method, QC samples were employed during batch procedure (Simader et al. 2015; Dunn et al. 2011). The variations in the intensity of variables were within 20%, which is acceptable (Triba et al. 2015). Overlaid TICs of QC samples analyzed throughout the run were performed to provide a visual examination of the performance of LC-TOF-MS system. QC samples showed that little variation throughout the whole analytical run and variations in intensity and retention time were acceptable, verifying good analytical conditions and providing a further assurance of data quality.

Multivariate Statistical Analysis and Chemical Marker Discovery

After extraction and filter, TICs from all samples divided into two groups revealed a number of features in total of 4505 and 4516, respectively. Then, by the analysis of software Sigma-p, as Fig. 1a shows, the score plot of unsupervised PCA of all three kinds of rhubarb samples showed a good clustering trend in the same category and a better differentiation among different species (DH-1, SDH-2, and TDH-3). The developed PCA model explained 77% of all variations in X and $Q^2 = 0.63$ that implied good predictive capability. In PCA score plot, SDH and TDH samples located more tightly than DH, since official rhubarb includes three kinds (*Rheum palmatum L.*, *Rheum officinale Baill.*, and *Rheum tanguticum Maxim.ex Balf.*) which have been researched that exist some difference in composition (Ye et al. 2007).

To investigate specifically discriminatory compounds contributing to differentiating official and unofficial rhubarb, supervised OPLS-DA were modeled based on the features filtered in two pairs, DH vs SDH and DH vs TDH, respectively. Two OPLS-DA models were well constructed regarding parameters $Q^2 = 0.983$ and $Q^2 = 0.981$. As it can be observed in Fig. 1b, c, variations in two areas (marked with a to z and A to I in upper right corner and lower left quarter) of two s-plot graphs were the most compounds serving for discriminant analysis by OPLS-DA, and therefore, these compounds should be considered as potential markers. Components with high dispersion degree and high VIP value gave a significant contribution for classification. For DH vs SDH and DH vs TDH two pairs, a total of 35 components were selected as candidates based on VIP value ($VIP > 1$) generated by SIMCA-P and cross-validated predictive residuals (CV-ANOVA) ($p < 0.01$). What is more, it is noteworthy while comparing all potential markers of two groups that markers with higher content in official rhubarb were semblable. This fact implied that these significant markers with higher content in authentic rhubarb and lower content in SDH and TDH were specific to official rhubarb. This result might be useful for inspecting rhubarb authenticity, and the category of suspicious rhubarb may be not limited to SDH and TDH.

Component Diversity in Official and Unofficial Rhubarb and Tentative Identification of Marker Compounds

The similarity analysis of total ion chromatograms was performed by “Similarity Evaluation System for Chromatographic Fingerprints of TCM” (Chinese Pharmacopoeia Commission, version 2004A). Results showed high similarity among the different batches of rhubarb belonging to the same category. Since 35 compounds were discriminant variables in DH, SDH, and TDH, these compounds were then selected from three batches (NO. 1, NO. 9, and NO. 14) among 21 samples as characteristic

markers to visually compare content differences and further confirm the unsubstitutability of official rhubarb. As shown in Fig. 4a–i, validation ions were extracted from their TICs and then combined to form extracted ion current chromatograms (EICs). Intuitively, peak number and ion intensity were significantly different in five types of chemical markers among DH (Fig. 4a, d, g, j), SDH (Fig. 4b, e, h, k), and TDH (Fig. 4c, f, i, l).

To assignment characteristic components, the screened 35 chemical markers were totally unambiguously/tentatively characterized, including anthraquinone glycosides, tannins, stilbenes, naphthalenes, and butyrophenones. The strategy for identifying marker compounds could be concluded in three procedures. Firstly, accurate mass was used to produce several possible molecular formulas (within a mass error of 5 ppm) by using Qualitative Analysis of MassHunter Acquisition Data B.04.00. The formula with the highest score was searched in SciFinder, and structures related to rhubarbs would be selected as candidates. The second step was to obtain fragments of candidates in a series of fragmentor voltages of MS-TOF, compare variation tendency, and propose probable fragmentation patterns. The final step was to compare experiment fragments with those in scientific literature for unequivocal structural validation since natural metabolites are complex and difficult to synthesize. Following the three steps, 35 marker compounds were all tentatively identified without the help of any reference substances. Table 1 reports retention time, m/z value, corresponding ions, calculated mass error, UV value, and assignment.

Markers in DH

Ten anthraquinone compounds including peak 22, peak 23, peak 26, peak 27, peak 28, peak 30, peak 32, 33, and peak 34, 45 were selected for extraction ion analysis. As shown in Fig. 4a–c, EIC chromatographs at m/z 417.11, 431.09, 459.09, 269.04, 517.09, 283.02, 297.04, 269.04, and 253.05 were combined to compare the content difference. Following the three steps, totally 10 anthraquinone markers tentatively identified, free anthraquinone compounds 32, 28, 34, 35 were tentatively identified as rhein, aloe-emodin, emodin, and chrysophanol, and their structures were confirmed by comparing accurate masses and fragment ions with those described in literatures (Yan et al. 2016). Here, peaks 23, 26, and 30 were used as examples for the stepwise illumination of the procedure of characterization. Based on the fragment ions of compounds 23 and 26, it was found that they all existed a loss of 162 Da (glucosyl residue); therefore, they were preliminarily concluded to be glucosides. Then, the quasi-molecular ion mass values of compounds 23 and 26 are $[M-H]^-$, $[2M-H]^-$, and $[M+Na]^+$ (m/z at 431.09, 863.2, 455.09), and the fragments $269.04[M-H-glucosyl]^-$, $241.05[269-H-CO]^-$, and $225.05[269-CO_2]^-$ which is the characteristic fragments of emodin indicated that they were isomers of emodin-O-glucoside. The fragments of compound 30 were with m/z at 517.09 $[M-H]^-$, 473.1 $[M-H-CO_2]^-$, 269.04 $[M-H-malonyl-glucosyl]^-$, and

Fig. 1 PCA score plot with the statistic parameters: $R^2X = 0.77$, $Q^2 = 0.63$ (a); S-plot of OPLS-DA model for DH versus SDH (b); S-plot of OPLS-DA model for DH versus TDH (c) (n(DH) = 8, n(TDH) = 8, n(SDH) = 5)

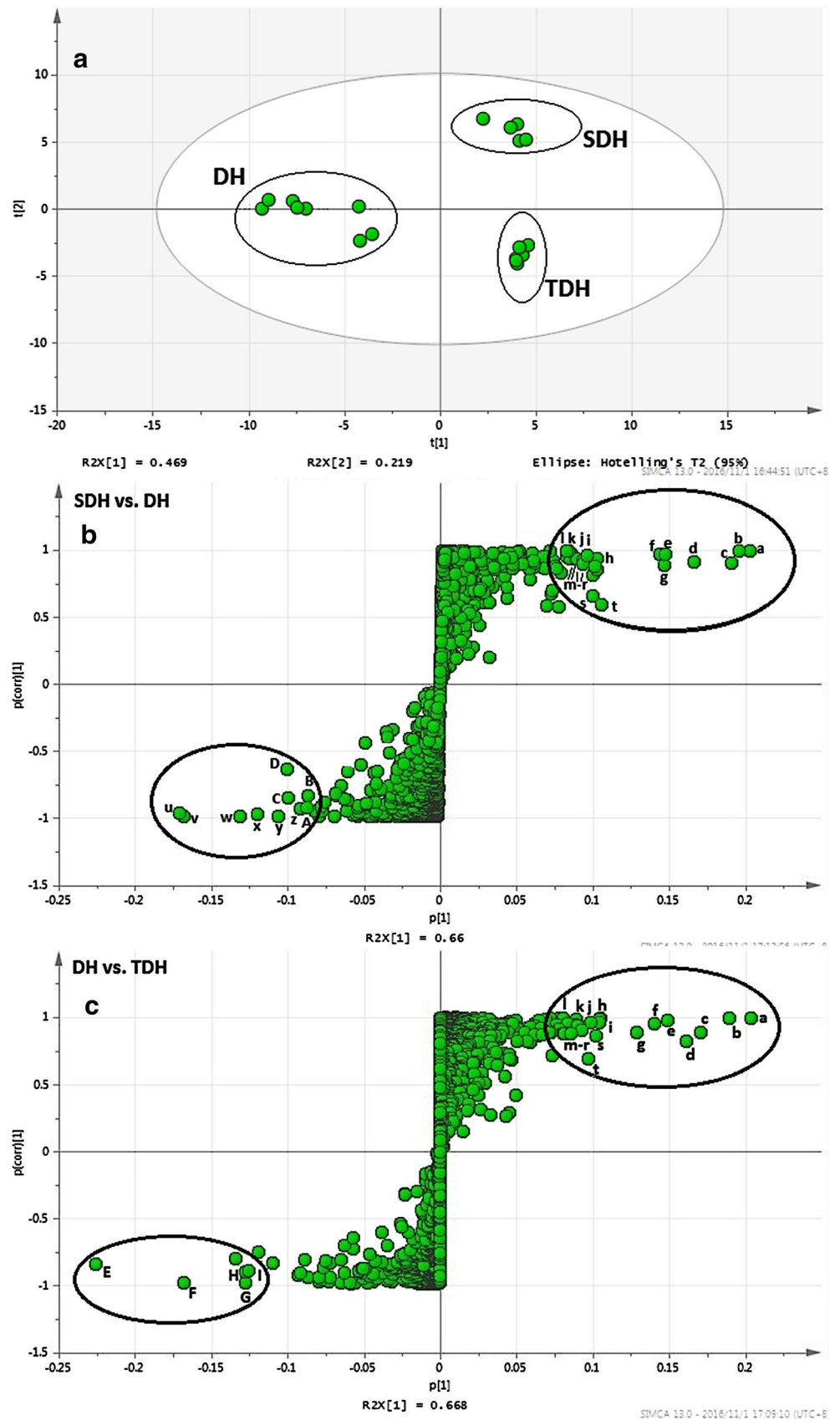


Table 1 Tentative identification of compounds in rhubarb extracts

No.	RT (min)	MF	MW	UV (nm)	Quasi-molecular ions (\pm ; ion ppm)	In source CID (TOF) (ion)	Assignment
1	11.313	C ₁₃ H ₁₆ O ₁₀	332	218,273	331.0680 ([M-H] ⁻ , -2.81)	169.0144 [M-H-glucosyl] ⁻ 125.0243 [169-CO ₂] ⁻ 125.0243 [M+H-CO ₂] ⁻	Galloyl-O-glucoside
2	12.146	C ₇ H ₆ O ₅	170	216,266	169.0146 ([M-H] ⁻ , -2.09)	425.0884 [M-H-C ₈ H ₈ O ₃] ⁻ 407.0789 [M-H-C ₈ H ₈ O ₃ -H ₂ O] ⁻ 289.0729 [M-H-catechin] ⁻ 245.0811 [289-CO ₂] ⁻	Galic Acid Procyanidin B
3	23.483 24.516 31.018	C ₃₀ H ₂₆ O ₁₂	578	202,209,272	577.1331 ([M-H] ⁻ , 3.55)	165.019 [M-H-C ₇ H ₆ O ₂] ⁻ 137.0247 [M-H-C ₈ H ₈ O ₃] ⁻ 125.024 [M-H-C ₉ H ₈ O ₃] ⁻ 577.13487 [M-H-galloyl] ⁻ 289.0684 [577-catechin] ⁻ 169.011 [gallic acid-H] ⁻ 125.0250 [169-CO ₂] ⁻	Epicatechin or Catechin
4	27.917	C ₁₅ H ₁₄ O ₆	290	223,271	289.071 ([M-H] ⁻ , 2.64)	243.0673 [M-H-glucosyl] ⁻ 225.0567 [243-H ₂ O] ⁻ 201.0567 [243-C ₂ H ₂ O ₂] ⁻ 175.041 [243-C ₂ H ₂] ⁻	Procyanidin B-O-gallate
5	32.218 34.669	C ₃₇ H ₃₀ O ₁₆	730	272	729.147 ([M-H] ⁻ , -1.22)	201.0567 [243-C ₂ H ₂ O ₂] ⁻ 175.041 [243-C ₂ H ₂] ⁻ 243.0642 [M-H-p-coumaroyl-glucosyl] ⁻ 225.0567 [243-H ₂ O] ⁻ 201.0567 [243-C ₂ H ₂ O ₂] ⁻ 307.0824 [M-H-243] ⁻ 145.0289 [307-glucosyl] ⁻	Piceatannol-O-Glucopyranoside
6	39.743 48.395	C ₂₀ H ₂₂ O ₉	406	301,317	405.1184 ([M-H] ⁻ , 1.74)	289.068 [M-H-galloyl] ⁻ 169.0144 [gallic acid-H] ⁻ 125.0250 [169-CO ₂] ⁻ 313.0576 [M-H-But] ⁻ 169.0143 [gallic acid-H] ⁻ 125.0250 [169-CO ₂] ⁻	Piceatannol-O-(6"-O-p-coumarate)-glucopyranoside
7	44.227	C ₂₉ H ₂₈ O ₁₁	552	312,323	551.1553 ([M-H] ⁻ , 1.06)	405.1173 [M-H-galloyl] ⁻ 313.071 [Galloyl-glucosyl] ⁻ 169.015 [313-H-glucosyl] ⁻ 125.025 [169-CO ₂] ⁻ 243.0642 [M-H-galloyl-glucosyl] ⁻ 225.0567 [243-H ₂ O] ⁻ 201.0567 [243-C ₂ H ₂ O ₂] ⁻ 175.041 [243-C ₂ H ₂] ⁻ 225 [243-H ₂ O] ⁻ 201.0567 [243-C ₂ H ₂ O ₂] ⁻ 175.041 [243-C ₂ H ₂] ⁻	Epicatechin/catechin-3-O-gallate
8	44.805	C ₂₂ H ₁₈ O ₁₀	442	223,271	441.0832 ([M-H] ⁻ , 1.09) 883.1709 ([2M-H] ⁻ , 2.06)	313.0576 [M-H-But] ⁻ 169.0143 [gallic acid-H] ⁻ 125.0250 [169-CO ₂] ⁻	Isolindleyin
9	47.089	C ₂₃ H ₂₆ O ₁₁	478	217,268	477.1420 ([M-H] ⁻ , -3.7)	405.1173 [M-H-galloyl] ⁻ 313.071 [Galloyl-glucosyl] ⁻ 169.015 [313-H-glucosyl] ⁻ 125.025 [169-CO ₂] ⁻	Piceatannol-O-(6"-O-galloyl)-glucopyranoside
10	50.812	C ₂₇ H ₂₆ O ₁₃	558	305,320	557.1307 ([M-H] ⁻ , -1.14)	243.0672 ([M-H] ⁻ , -3.78)	Piceatannol
11	52.596	C ₁₄ H ₁₂ O ₄	244	301,317	243.0672 ([M-H] ⁻ , -3.78)	175.041 [243-C ₂ H ₂] ⁻ 257.0841 [M-H-glucosyl] ⁻ 242.0566 [257-CH ₃] ⁻ 224.0451 [242-H ₂ O] ⁻ 313.0565 [M-H-C ₉ H ₁₀ O ₂] ⁻ 169.0146 [gallic acid-H] ⁻	Rhapontigenin-O-glucopyranoside
12	55.397	C ₂₁ H ₂₄ O ₉	420	286,325	419.1354 ([M-H] ⁻ , -1.54)		1-Galloyl-2-benzenepropanoate- β -D-glucopyra
13	59.659	C ₂₂ H ₂₄ O ₁₁	464	212,280	463.1223 ([M-H] ⁻ , 4.93)		

Table 1 (continued)

No.	RT (min)	MF	MW	UV (nm)	Quasi-molecular ions (\pm ; ion ppm)	In source CID (TOF) (ion)	Assignment
14	62.227	C ₂₇ H ₂₆ O ₁₂	542	218,292	541.1341 ([M-H] ⁻ , 1.94)	125.0248 [169-CO ₂] ⁻ 313.0567 [M-H-227] ⁻ 227.0733 [Res] ⁻ 169.077 [gallic acid-H] ⁻ 125.0250 [169-CO ₂] ⁻	noside Resveratrol-4'-O-β-D-(6''-O-galloyl)-glucopyranoside
15	63.594	C ₁₉ H ₂₂ O ₉	394	230,256,317	393.12 ([M-H] ⁻ , -2.27)	231.0672 [M-H-glucosyl] ⁻ 188.0419 [231-COCH ₃] ⁻	6-Hydroxymusizinin-O-glucopyranoside
16	66.037	C ₂₂ H ₂₂ O ₁₁	462	218,282	461.1077 ([M-H] ⁻ , 2.68)	313.0534 [M-H-cinnamoyl] ⁻ 169.0149 [gallic acid-H] ⁻ 125.0250 [169-CO ₂] ⁻	cinnamoyl-O-galloyl-glucopyranoside
17	66.233	C ₂₈ H ₂₈ O ₁₃	572	297,338	571.1455 ([M-H] ⁻ , 0.38)	257 [M-H-galloyl-glucosyl] ⁻ 313.071 [galloyl-glucosyl] ⁻ 169.015 [313-H-glucosyl] ⁻ 125.025 [169-CO ₂] ⁻	Rhapontigenin-O-(6''-O-galloyl)-glucopyranoside
18	71.785	C ₁₅ H ₁₄ O ₄	258	286,325	257.081 ([M-H] ⁻ , 3.63)	242.057 [M-CH ₃] ⁻ 224.0453 [242-H ₂ O] ⁻	Rhapontigenin or isorhapontigenin
19	77.287	C ₁₉ H ₂₂ O ₈	378	225,263,336	377.1240 ([M-H] ⁻ , 0.51)	199.0755 [M-C ₂ H ₂ O ₂] ⁻ 215.034 [M-H-glucosyl] ⁻ 187.0446 [215-CO] ⁻	Musizinin-O-glucopyranoside
20	77.464	C ₂₉ H ₂₆ O ₁₅	614	210,273	613.1169 ([M-H] ⁻ , 4.88)	159.0472 [187-CO] ⁻ 461.1077 [M-H-galloyl] ⁻ 443.1001 [M-H-galloyl-H ₂ O] ⁻	Cinnamoyl-di-O-galloyl-glucoside
21	78.77	C ₂₁ H ₂₄ O ₈	404	286,325	403.1385 ([M-H] ⁻ , 3.33) 807.2855 (2 M-H ⁻ , 1.81)	465.0679 [M-H-cinnamoyl] ⁻ 169.0149 [gallic acid-H] ⁻ 125.0250 [169-CO ₂] ⁻	Desoxyrhapontigenin-O-glucopyranoside
22	79.838	C ₂₁ H ₂₂ O ₉	418	260,350	835.2449 (2 M-H ⁻ , 0.7) 441.1171 ([M + Na] ⁺ , -3.39)	241.0833 [M-H-glucosyl] ⁻ 226.0592 [241-CH ₃] ⁻ 255.0695 [M-H-glucosyl] ⁻ 227.077 [255-CO] ⁻	Alion
23	82.432	C ₂₁ H ₂₀ O ₁₀	432	218,274,430	431.0969 ([M-H] ⁻ , 3.41) 863.2075 (2 M-H ⁻ , -4.03) 455.0933 ([M + Na] ⁺ , 3.45)	269.0482 [M-H-glucosyl] ⁻ 241.0528 [269-CO] ⁻ 225.0502 [269-CO ₂] ⁻	Emodin-1-O-β-D-glucopyranoside
24	83.738	C ₂₀ H ₂₄ O ₉	408	230,256,317	407.136 ([M-H] ⁻ , -3.06)	245.0813 [M-H-glucosyl] ⁻ 230.0620 [M-H-CH ₃] ⁻ 215.0725 [215-CH ₃] ⁻ 187.0438 [215-CO] ⁻ 159.0452 [187-CO] ⁻ 131.0521 [159-CO] ⁻	Torachryson-8-O-β-D-glucopyranoside
25	86.556	C ₂₈ H ₂₈ O ₁₂	556	286,325	555.1521 ([M-H] ⁻ , -2.34)	313.0679 [galloyl-glucosyl] ⁻ 169.0143 [313-H-glucosyl] ⁻ 125.025 [169-CO ₂] ⁻	Desoxyrhapontigenin-O-(6''-O-galloyl)-glucopyranoside
26	96.136	C ₂₁ H ₂₀ O ₁₀	432	274,218,430	431.0968 ([M-H] ⁻ , 3.64) 863.2039 (2 M-H ⁻ , -4.03) 455.0926 ([M + Na] ⁺ , 4.98)	269.0483 [M-H-glucosyl] ⁻ 241.0593 [269-CO] ⁻ 225.0536 [269-CO ₂] ⁻	Emodin-8-O-β-D-glucopyranoside

Table 1 (continued)

No.	RT (min)	MF	MW	UV (nm)	Quasi-molecular ions (\pm ; ion ppm)	In source CID (TOF) (ion)	Assignment
27	97.52	C ₂₂ H ₂₀ O ₁₁	460	217,251,430	459.0933 ([M-H] ⁻ , 0.03) 919.1901 ([2 M-H] ⁻ , 4.08) 483.0885 ([M + Na] ⁺ , 2.65) 269.0448 ([M-H] ⁻ , 2.78) 293.0435 ([M + Na] ⁺ , -4.97)	399.1092 [M-H-OCO ₂] ⁻ 253.0504 [M-H-carboxyl-glucosyl] ⁻ 225.0574 [253-CO] ⁻ 239.044 [M-H-CH ₂ O] ⁻ 223.029 [M-H-CH ₂ O ₂] ⁻ 195.045 [M-H-C ₂ H ₂ O ₃] ⁻ 183.0413 [M-H-C ₃ H ₂ O ₃] ⁻ 167.054 [M-H-C ₃ H ₂ O ₄] ⁻ 187.0449 [215-CO] ⁻ 159.0459 [187-CO] ⁻ 131.0514 [159-CO] ⁻ 473.1071 [M-H-CO ₂] ⁻ 269.0445 [M-H-malonyl-glucosyl] ⁻ 225.0551 [269-CO ₂] ⁻ ,	Chrysophanol-8-O-(6'-carboxyl)-glucopyranoside Aloecmodin Musizin Emodin-8-O-(6'-O-malonyl)-glucopyranoside 6-Methoxymusizin
28	110.39	C ₁₅ H ₁₀ O ₅	270	221,250 274,430			
29	111.574	C ₁₃ H ₁₂ O ₃	216	225,263,336	215.0721 ([M-H] ⁻ , -3.4)		
30	118.776	C ₂₄ H ₂₂ O ₁₃	518	218,274,430	517.0967 ([M-H] ⁻ , 3.99) 1035.207 ([2 M-H] ⁻ , -2.12) 519.1157 ([M + H] ⁺ , -4.59) 541.0926 ([M + Na] ⁺ , 4.92) 245.0814 ([M-H] ⁻ , -3.4)		
31	121.51	C ₁₃ H ₁₂ O ₃	246	230,256,317			
32	124.044	C ₁₅ H ₈ O ₆	284	232,260,410	283.0233 ([M-H] ⁻ , 1.81)		
33	124.694	C ₁₆ H ₁₀ O ₆	298	230,258,410	297.041 ([M-H] ⁻ , -1.81) 299.0544 ([M + H] ⁺ , 2.05) 321.0368 ([M + Na] ⁺ , 0.5) 269.0448 ([M-H] ⁻ , 2.78) 293.0476 ([M + Na] ⁺ , 1.52)		1-Methyl-2,8-di-hydroxy-3-carboxyl-9,10-anthraquinone Emodin
34	136.881	C ₁₅ H ₁₀ O ₅	270	220,250			
35	137.948	C ₁₅ H ₁₀ O ₄	254	219,250,410	253.0503 ([M-H] ⁻ , 1.31)		Chrysophanol

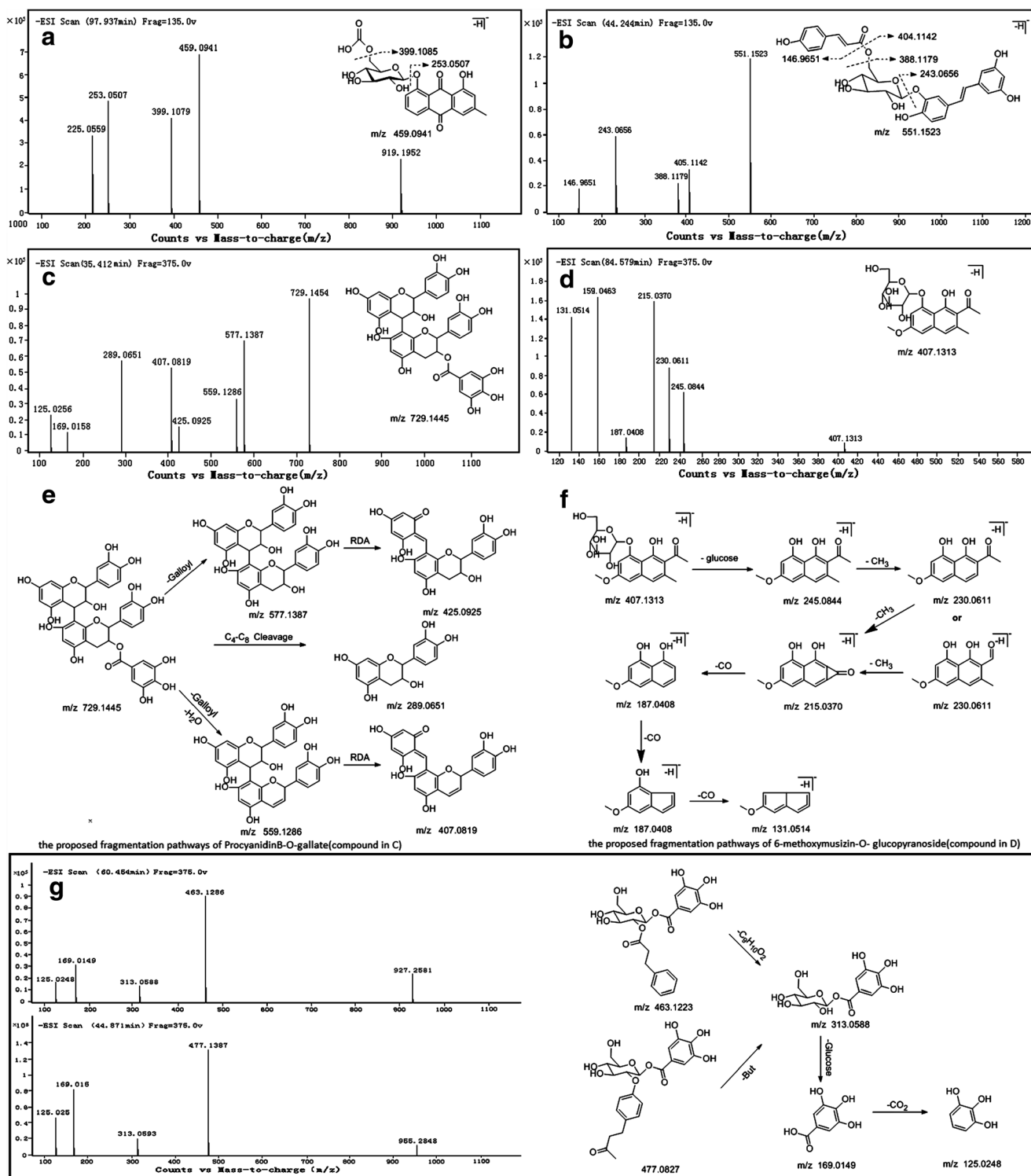


Fig. 2 The TOF-MS spectra and proposed fragmentation pathways of chrysophanol-O-(6'-O-carboxyl)-glucoside (a), piceatannol-O-(6''-O-p-coumaroate)-glucopyranoside (b), procyanidin B-O-gallate (c), 6-methoxymusizin-O-glucopyranoside (d), the detailed fragmentation

pathway of procyanidin B-O-gallate (e), the detailed fragmentation pathway of 6-methoxymusizin-O-glucopyranoside (f), isolindleyin, 1-galloyl-2-benzenepropanoate-β-D-glucopyranoside and the detailed fragmentation pathway (g) in Negative ion mode

225.05, i.e., neutral loss of 44 Da and 248 Da which were the diagnostic fragmentation of malonyl-glucoside (Ye et al. 2007). Therefore, it was tentatively assigned as emodin-O-(6'O-

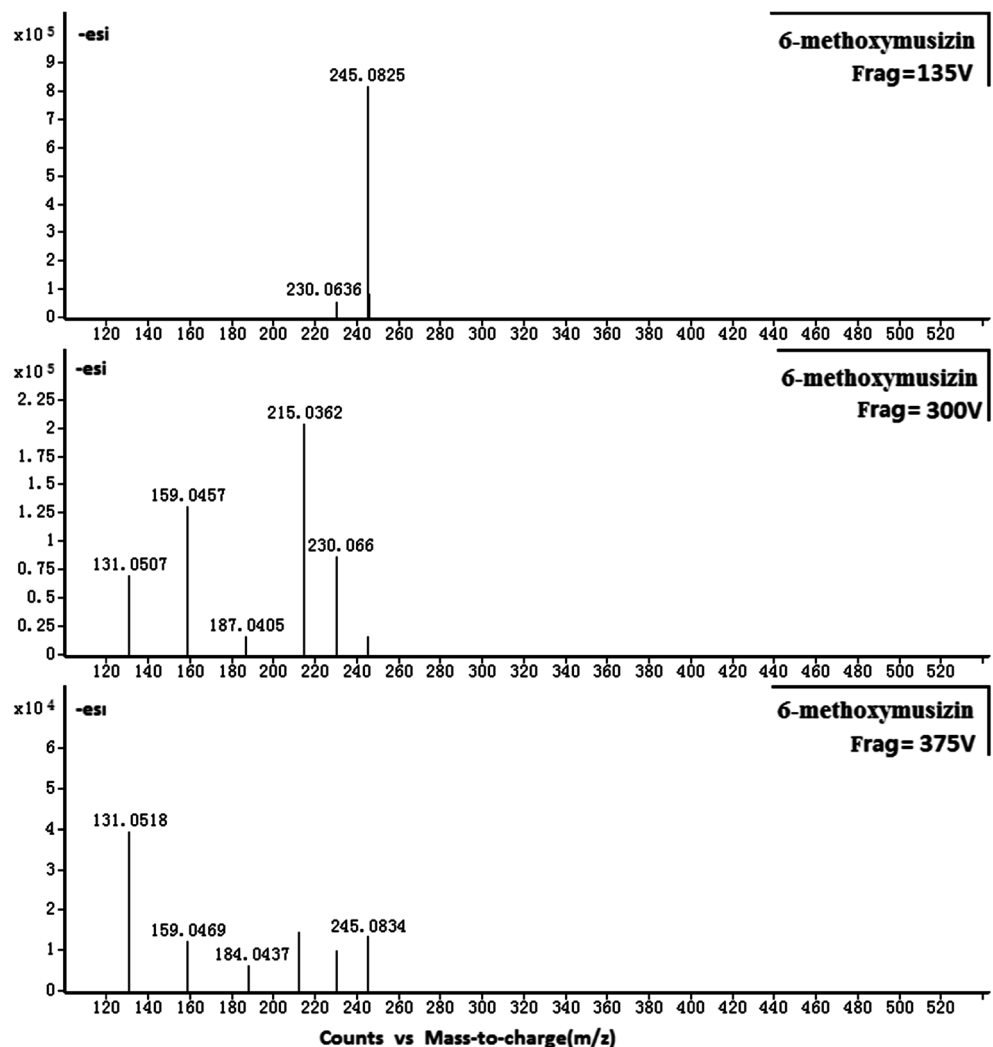
amlyl)-glucoside. Similarly, peak 27 exhibited ions with m/z at 459[M-H]⁻, 399, and 253, i.e., neutral loss of 60 and 206 Da which were carboxyl-glucoside and CO₃ unit. Thus, it was

tentatively assigned as chrysophanol-O-(6'-O-carboxyl)-glucoside. The proposed fragmentation pathway and TOF-MS spectrum of compound 27 is showed in Fig. 2a. In addition, UV maximum absorption wavelengths of 10 anthraquinones were at about 240–290 and 430–440 nm, which were consistent with the characteristic absorption of anthraquinones. According to TOF-MS identification results, anthraquinone glucosides were the common metabolites of three species of DH, and their retention time fell in between 70 and 140 min. The relative content of these common compounds was compared in terms of relative ion intensity of corresponding peaks. Typically, compared with DH, the total relative ion intensity values of peaks 23, 26, 27, 30, and 33 (anthraquinone glucosides) in the chromatograms of SDH and TDH were about 50.8 and 23.5%, while it was found that SDH contained more emodin-O- β -D-glucopyranoside than DH.

Tannins and butyrophenones, the retention time of which fell in between 0 and 80 min and was the common type of metabolites contained in three species of rhubarb, were also chosen to make a comparison. By comparing the relative content of these common compounds in terms of peak areas of peak 1, peak 2, peak 4, peak

5, and so on (Fig. 4d–f). The results indicated that tannins-related components were the main common compounds in three species of rhubarb, and SDH and TDH contained less amount and fewer types of tannins than DH. The UV maximum absorption bands of tannins were at 200–220 and 260–270 nm. Based on the accurate mass values and fragmentation pattern of MS, a total of eight tannin category compounds were tentatively identified. Compounds 4 and 2 were identified as epicatechin/catechin and gallic acid, respectively, based on accurate mass values and fragmentation patterns as earlier researched in our laboratory (Yan et al. 2016). In addition, the fragments of ions at m/z 169 [gallic acid-H]⁻, 125 [169-CO₂]⁻, and 124 in fragmentor of 375 V are characteristic fragments of gallic acid. In the spectrum, compound 3 showed fragment ions at m/z 577, 425, 407, 289, and 245, which were consistent with the previous study (Gu et al. 2003); thus, it was tentatively identified as Procyanidin B. The main tannin markers were gallic acid and its gallate (peaks 5, 8, 16, and 20) or gallic acid glycosides (peak 1). The proposed fragmentation pathway and MS-TOF spectrum of procyanidin B-O-gallate are presented in Fig. 2c, e. Based on accurate mass values and

Fig. 3 The TOF-MS spectra of Torachryson in the fragmentor of 135, 300, and 375 V



fragmentation patterns, two butyrophenones were tentatively identified. Peaks 9 and 13 showed the same series of fragments at m/z 313, 169, and 125, which showed that they belonged to galloyl glucopyranoside and were consistent with tannin cleavage pattern. Then, compound 9 and compound 13 gave a benzyl butyl ketone group and $C_9H_{10}O_2$ unit to generate ions at m/z 313. By combining their accurate mass values and polarity, they were tentatively identified as isolindleyin and 1-galloyl-2-benzenepropanoate- β -D-glucopyranoside. The proposed fragmentation pathway and TOF-MS spectrum of compounds 34 and 35 are presented in Fig. 2g.

Markers in SDH

A high content of stilbenes including peaks 6, 7, 10, 11, 12, 14, 17, 18, 21, and 25 were contained in SDH (Fig. 4g–i) and were not detected in DH except peak 14. Stilbenes were the major composition from SDH; in this study, based on elemental composition and fragmentation behaviors, a total of 10 stilbene markers were tentatively identified. Compounds 11 and 18 were identified as piceatannol and rhapontigenin or iso-rhapontigenin based on accurate mass values, fragments, and literature (Borniquez 2009). Compound 12 generated fragments at m/z 419 $[M-H]^-$ and 257 in negative mode; so, it was deduced to be a glucosyl group bonded to rhapontigenin or isorhapontigenin. In the same way, peaks 6, 7, and 21 were all tentatively identified as stilbene glucosides. Compounds 17 and 10 possessed the same fragments at m/z 313, 169, and 125 in fragmentor of 375 V, which were characteristic ion of galloyl-glucopyranoside; then, the other fragments were with m/z at 557 $[M-H]^-$, 243 and 571 $[M-H]^-$, 257,

respectively. Thus, peaks 17 and 10 were tentatively assigned as rhapontigenin-O-(6''-O-galloyl)-glucopyranoside or isorhapontigenin-O-(6''-O-galloyl)-glucopyranoside and piceatannol-O-(6''-O-galloyl)-glucopyranoside. Similarly, the characterization of compounds 14 and 25 was carried out, and they were tentatively identified as resveratrol-4'-O- β -D-(6''-O-galloyl)-glucopyranoside and desoxyrhapontigenin-O-(6''-O-galloyl)-glucopyranoside.

Proposed fragmentation pathway and TOF-MS spectrum of compound 7 are presented in Fig. 2b. In respect of pharmacological effects of them, previous studies demonstrated that piceatannol (peak 11) can suppress the activation of some transcription factors and exhibit potential anticancer properties as suggested by its ability to suppress proliferation of a wide variety of tumor cells, including leukemia, cancers of the breast, melanoma, and so on (Piotrowska et al. 2012). Additionally, rhaponticin (peak 12) is a prodrug that has extensive antiallergic and antithrombotic properties (Park et al. 2002).

Markers in TDH

Peaks 15, 29, and 31, the peaks, of which were striking, could be typical chemicals in TDH (Fig. 4j–l). Particularly, the data showed that DH contained 1.3% of peak 29 of TDH in the means of relative ion intensity, and peak 19 was not detected in DH. According to TOF-MS spectra, five naphthalene derivative markers were identified. In fragmentor of 375 V, peak 31 generated ions at m/z 230 and 215, which were the successive loss of two methyl groups from ion at m/z 245. Then, ions

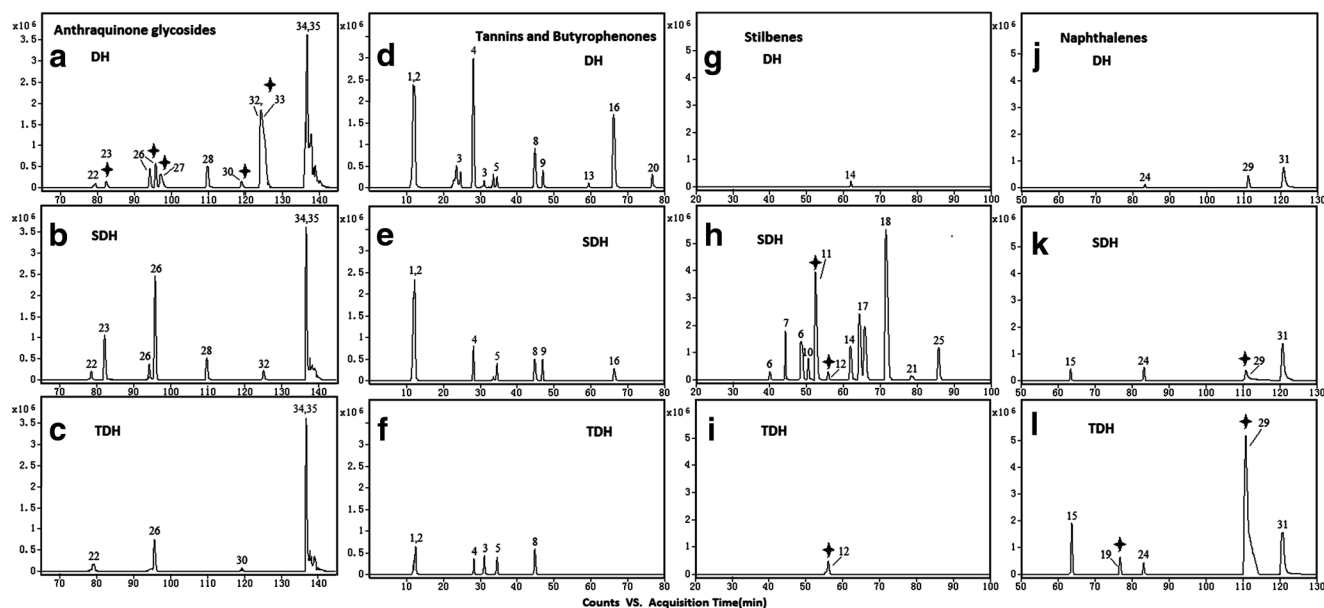


Fig. 4 The extracted ion chromatograms (EICs) of anthraquinone glycosides in DH (a), SDH (b), TDH (c), tannins and butyrophenones in DH (d), SDH (e), TDH (f), stilbenes in DH (g), SDH (h), TDH (i), and

naphthalene derivatives in DH (j), SDH (k), TDH (l). Peaks marked with four corner stars expressed markers with specific pharmacological activities

at m/z 187, 159, and 131 were the successive loss of three CO groups from ion at m/z 215. The fragmentation pattern was typical to 6-methoxymusizin. Corresponding MS spectrums of peak 31 in fragments of 135, 300, and 375 V are showed in Figs. 3 and 4. The dynamic variation that fragments regularly increased with the increase of fragment voltage could provide more chemical compound fragment information during identification, and optimization of fragment voltage is particularly important. Compared to fragments of compound 31, the fragments of compound 29 lack an ion at m/z 230; thus, it was suggested to be musizin. Compounds 19 and 24 yielded fragments at m/z 377, 215 and 407, 245, i.e., a neutral loss of 162 Da, indicating that they were glucosides. Their mass-to-charge ratios of aglycone are in alignment with musizin and 6-methoxymusizin; so, they were deduced to be musizin-O-glucopyranoside and 6-methoxymusizin-O-glucopyranoside. TOF-MS spectrum and proposed fragmentation pathway of compound 24 are presented in Fig. 2d, f. Compound 15 generated fragments at m/z 393, 231, and 215, i.e., a neutral loss of hydroxyl and glucosyl; so, it was tentatively speculated to be 6-hydroxylmusizin-O-glucopyranoside. In the aspect of pharmacological functions, musizin, once isolated from New Zealand flax, has useful antifungal, antibacterial, and anticancer activities (Harvey and Waring 1987). Musizin-O-glucopyranoside can induce apoptosis via the activation of caspases-3 and -7 in Hela cell (Yong et al. 2010).

The Comparison of Pharmacological Activities Between Official and Unofficial Rhubarb

In the aspect of pharmacological functions, given that purgative components in official rhubarb are scrupulously researched as anthraquinone glycosides, remarkable percentage reduction of which in unofficial rhubarb would inevitably decrease the diarrhea and purgative effect of rhubarb. Additionally, previous studies demonstrated that piceatannol can suppress the activation of some transcription factors and exhibit potential anticancer properties as suggested by its ability to suppress proliferation of a wide variety of tumor cells, including leukemia, cancers of the breast, melanoma, and so on (Piotrowska et al. 2012). Furthermore, rhaponticin is a prodrug that has extensive anti-allergic and antithrombotic properties (Park et al. 2002). As for TDH, musizin, once isolated from New Zealand flax, has useful antifungal, antibacterial, and anticancer activities (Harvey and Waring 1987). Musizin-O-glucopyranoside can induce apoptosis via the activation of caspases-3 and -7 in Hela cell (Yong et al. 2010). In current study, these stilbene and naphthalene distinction markers showed a relatively higher amount in unofficial rhubarb when compared with that of official rhubarb. Therefore, the possible pharmacological activities of SDH and TDH were deduced to be

anticancer, antifungal, and antibacterial, which significantly differ with DH.

Conclusion

A HPLC-DAD-TOF/MS coupled with the use of PCA and OPLS-DA method was successfully developed to discriminate official and unofficial rhubarb. Based on the accurate mass value of a series of fragments under different fragmentors of MS and the reference of literatures, 35 differential markers were unambiguously or tentatively identified. Unofficial rhubarb including SDH and TDH showed significant decrease in the content of anthraquinone glycosides, which are mainly responsible for the purgative activity of rhubarb. Stilbenes and naphthalenes, the major constituents of SDH and TDH, have mainly pharmacological activities of anti-cancer and antifungal. So, this experiment has guiding significance to a certain that during clinical medication, official rhubarb could not be mixed or replaced with SDH and TDH. In the comparison of DH vs SDH and DH vs TDH, authenticity markers with higher content in official rhubarb were the same; thus, these markers may be used in the future to detect rhubarb adulteration regardless of the variety of rhubarb to be tested and to be one step ahead of fraudsters in the herb market. Also, these markers could be used to conduct adulteration identification in herb medicine market regardless of the approach employed.

Acknowledgements This research was financially supported by the National Natural Science Foundation of China (No. 81274063) and a Project Funded by the Priority Academic Program Development of Jiangsu Higher Education Institutions.

Compliance with Ethical Standards

Conflict of Interest Shuzhen Xu declares that he has no conflict of interest. Gongjun Yang declares that he has no conflict of interest. Fang Feng declares that he has no conflict of interest.

Ethical Approval This article does not contain any studies with human participants or animals performed by any of the authors.

Informed Consent Not applicable.

References

- Bajic JE, Eden GL, Lampton LS et al (2016) Rhubarb extract partially improves mucosal integrity in chemotherapy-induced intestinal mucositis. *World J Gastroenterol* 22:8322–8333
- Borniquez G (2009) Changes in chemical composition of a red wine aged in acacia, cherry, chestnut, mulberry, and oak wood barrels. *J Agric Food Chem* 57:1915–1920

- Cai Z, Lee FSC, Wang XR et al (2002) A capsule review of recent studies on the application of mass spectrometry in the analysis of Chinese medicinal herbs. *J Mass Spectrom* 37:1013–1024
- Chinese Pharmacopoeia commission (2015) Pharmacopoeia of the People's republic of China, vol 1. China Medical Science Press, Beijing, pp 23–24
- Chung KT, Wong TY, Wei CI et al (1998) Tannins and human health: a review. *Crit Rev Food Sci Nutr* 38:421–464
- Dunn WB, Broadhurst D, Begley P et al (2011) Procedures for large-scale metabolic profiling of serum and plasma using gas chromatography and liquid chromatography coupled to mass spectrometry. *Nat Protoc* 6:1060–1083
- Feng TS, Wang YG, Chai YS et al (2012) Comparison between *Rheum palmatum* L. and *Rheum franzenbachii* munt. On pharmacological effect and toxicity. *World Sci Technol Mod Tradit Chin Med Mater Med* 14:1863–1870
- Feng TS, Yuan ZY, Yang RQ et al (2013) Purgative components in rhubarbs: adrenergic receptor inhibitors linked with glucose carriers. *Fitoterapia* 91:236–246
- Gu L, Kelm MA, Hammerstone JF et al (2003) Liquid chromatographic/electrospray ionization mass spectrometric studies of proanthocyanidins in foods. *J Mass Spectrom* 38:1272–1280
- Harvey HE, Waring JM (1987) Antifungal and other compounds isolated from the roots of New Zealand flax plants (the genus *Phormium*). *J Nat Prod* 50:767–767
- Jelassi B, Anghelin M, Chamouton J et al (2013) Anthraquinone emodin inhibits human cancer cell invasiveness by antagonizing P2X7 receptors. *Carcinogenesis* 34:1487–1496
- Lastra CADL, Villegas I (2005) Resveratrol as an anti-inflammatory and anti-aging agent: mechanisms and clinical implications. *Mol Nutr Food res* 49:405–430
- Li YS, Tang J, Diao PY et al (2012) The distinctions between Dahuang and Shandahuang. *Chin J Vet Drug* 46:53–54
- Pang Y, Sun L, Jin HY et al (2014) Identification and quality evaluation of radix et Rhizoma Rhei by HPLC fingerprint and chemometrics analysis. *J Chin Pharm Sci* 49:287–293
- Park EK, Choo MK, Yoon HK et al (2002) Antithrombotic and antiallergic activities of rhaponticin from rhei rhizoma are activated by human intestinal bacteria. *Arch Pharm res* 25:528–533
- Piotrowska H, Kucinska M, Murias M (2012) Biological activity of piceatannol: leaving the shadow of resveratrol. *Mutat Res Rev Mutat Res* 750:60–82
- Santana DB, Costa RCD, Araújo RM et al (2015) Activity of Fabaceae species extracts against fungi and Leishmania: vatacarpan as a novel potent anti-Candida agent. *Rev Bras* 25:401–406
- Simader AM, Kluger B, Neumann NK et al (2015) QCScreen: a software tool for data quality control in LC-HRMS based metabolomics. *BMC Bioinf* 16:1–9
- Smith CA, Want EJ, O'Maille G et al (2006) XCMS: processing mass spectrometry data for metabolite profiling using nonlinear peak alignment, matching, and identification. *Anal Chem* 78:779–787
- Suboj P, Babykutty S, Valiyaparambil Gopi DR et al (2012) Aloe emodin inhibits colon cancer cell migration/angiogenesis by downregulating MMP-2/9, RhoB and VEGF via reduced DNA binding activity of NF- κ B. *Eur J Pharm Sci* 45:581–591
- Triba MN, Le ML, Amathieu R et al (2015) PLS/OPLS models in metabolomics: the impact of permutation of dataset rows on the K-fold cross-validation quality parameters. *Mol BioSyst* 11:13–19
- Yan Y, Zhang Q, Feng F (2016) HPLC-TOF-MS and HPLC-MS/MS combined with multivariate analysis for the characterization and discrimination of phenolic profiles in non-fumigated and sulfur-fumigated rhubarb. *J Sep Sci* 39:2667–2677
- Ye M, Han J, Chen H et al (2007) Analysis of phenolic compounds in rhubarbs using liquid chromatography coupled with electrospray ionization mass spectrometry. *J Am Soc Mass Spectrom* 18:82–91
- Yong Y, Shin SY, Lee Y et al (2010) A compound isolated from *Rumex Japonicus*, induces apoptosis in HeLa cells. *Appl Biol Chem* 53(5): 657–660
- Zhang L, Liu HY, Qin LL et al (2015) Global chemical profiling based quality evaluation approach of rhubarb using ultra performance liquid chromatography with tandem quadrupole time-of-flight mass spectrometry. *J Sep Sci* 38:511–522
- Zhu JJ, Wang ZT, Zhang CF et al (2008) Advances in studies on chemical components in plants of *Rumex L.* and their pharmacological activities. *Chin Tradit Herb Drug* 39:450–454